Measurements of Charge-to-Mass Ratios on Individual Blowing Snow Particles

D.S. Schmidt[1], J.D. Dent[1], R.A. Schmidt[2]
[1]Department of Civil Engineering, Montana State University, Bozeman, Montana 59717
[2]US Forest Service Rocky Mountain Forest and Range Experiment Station
222 South 22nd Street, Laramie, Wyoming 82070

ABSTRACT

Determining the electrostatic force acting on saltating snow particles requires knowledge of the electric field in the saltation region and the charge on the particle. To date, measurements of average charge-to-mass ratios for blowing snow samples have been made, but Schmidt and Schmidt (1992) indicate these may underestimate charge-to-mass ratios for individual particles, due to a mixture of positive and negative charge in the samples. This paper reports on measurements of charge-to-mass ratio for individual blowing snow particles during a moderate blowing snow storm in S.W. Wyoming. We measured charge-to-mass ratios as large as -208 mC/kg, significantly higher then the -10 mC/kg measured by Latham and Montagne (1977) and -50 mC/kg measured by Whishart (1969). This large charge-to-mass ratios was accompanied by a distribution of positive and negative charge on the particles, supporting the conclusions of Schmidt and Schmidt (1992).

INTRODUCTION

Wind is an incredibly powerful force capable of moving vast quantities of snow during blizzards. Deposition of wind blown snow forms large drifts that hamper winter travel. In mountainous regions, cornices and wind deposited snow in the lee of ridges trigger avalanches that damage structures and transport systems. Effective control of these natural phenomenon requires a better understanding of the physical processes in blowing snow.

Wind transports snow by three mechanisms. Particles roll along the surface in a process termed creep. This mechanism occurs in light winds and accounts for very little transport. Strong winds eject particles from the surface in a mode of transport called saltation. Particles in saltation bounce along the surface, rebounding to heights typically within 10 cm of the surface. Much of transport during blowing snow storms moves in saltation. In the third transport mode, known as suspension, particles travel without impact, at height that may extend several hundred meters in polar storms. Saltating particles are the source for suspended transport, therefore understanding saltation is essential to controlling blowing snow.

This paper reexamines the magnitude of the electrostatic charges that develop on saltating snow particles. Most laboratory and field studies of saltation have ignored electrostatic forces. In the few studies directed toward measuring particle charge, we believe the methods underestimate magnitudes. The remainder of this introduction presents a brief review of research on the electrostatic force and why previous experiments might underestimate particle charge-to-mass ratios. Following sections describe the equations, apparatus, field procedures, and results of our experiment. Our thoughts on the implications of the results on the saltation process are in the discussion.

THE SALTATION PROCESS

Saltating snow particles rebound from elastic impact with the surface, following long, low trajectories in response to forces of fluid drag and gravitation. Whether it be snow particles in the atmosphere, or glass beads in a wind tunnel, the equations that describe the motion of saltating particles are the same. White and Schultz (1977) used a high speed camera to photograph trajectories of saltating glass spheres in a wind tunnel. They found trajectories higher and longer then those predicted from theoretical equations involving only fluid drag and the gravitational force. This indicated the presence of an additional lift force. Lift develops if the particle spins and White and Schultz showed good agreement with the observed trajectories by adding the Magnus lift to the theoretical equations. To produce consistent trajectories from the addition of Magnus effect alone, White and Schultz assumed spin rates in the range 100 - 300 rev/s. Another force that could explain the additional lift on saltating particles is the electrostatic force that results from friction between the moving particles and the surface.

ELECTRIFICATION OF BLOWING SNOW

A charged particle, in an electric field, is subject to an electrostatic force. The magnitude of the force is equal to the product of the electric field and the charge on the particle. The force acts along the electric field vector, in the direction determined by the sign of the particle charge. Schmidt and Schmidt (1992) review the research on the mechanisms that produce charge separation in saltating snow. These mechanisms usually produce moving particles that are negatively charged, while surface particles become positive. Blizzard measurements (Schmidt, 1994) confirmed predictions by Schmidt and Dent (1993) that electric fields near the surface in saltating snow are several orders of magnitude larger than the fair- weather field (100 V/m).

Whishart (1968) and Latham and Mongtagne (1970) reported measurements of average charge-to-mass ratios in which samples of drifting particles were collected. Schmidt and Schmidt (1992) also reported charge and mass for blizzard particles collected in a portable Faraday cage, with simultaneous wind speed measurements. Reductions, and actual reversal, in sign of measured charge during wind gusts strongly suggested that eroded surface particles of opposite sign were mixing with moving particles. This would indicate average particle charge-to-mass ratio determined by measuring the charge on blowing snow samples and dividing by sample mass would underestimate charge-to-mass ratios of the individual snow particles.

EXPERIMENT OUTLINE

The purpose of the experiment presented here was to measure the charge-to-mass ratio on an individual blowing snow particle. In his famous experiment, Millikan (1910) measured the charge of single electrons from the motion of oil drops moving in a constant electric field. Camp (1977) used a variation on this technique to determine charge-to-mass ratios for falling snow crystals. Based on their methods we designed the apparatus and experiment described below to measure the the charge on drifting particles. Snow particles were extracted from saltation by a drift trap. Particles that did not impact the trap dropped vertically through a still air chamber containing a constant horizontal electric field. A detector triggered a photographic imaging system that produced photographs showing particle path and location at known time intervals . Charged particle are deflected horizontally by an amount proportional to their charge, with direction determined by the charge sign. Photographs showing deflection both left and right would confirm our hypothesis that positive and negative charged particles are transported simultaneously in saltation. The charge-to-mass ratio of the particle can be determined from these images using equations derived in the next section.

EQUATIONS OF MOTION

A charged particle falling through still air, with a horizontal electric field, is acted upon by the gravitational force, an electrostatic force, and a drag force due to air resistance that opposes the particles motion. If the direction the particle travels is defined by an angle q with the vertical (figure 1), the equations that describe the particle's motion are

$$F_E - F_d \sin\theta = m\ddot{x} \qquad (1)$$

and

$$mg - F_d \cos\theta = m\ddot{y} \qquad (2)$$

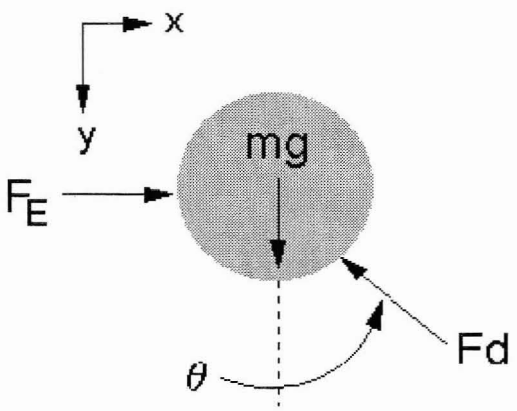

Figure 1: Free-body diagram of particle falling in air, subject to a constant electrostatic force.

The magnitude of the electrostatic force is $F_E = qE$, where E is the magnitude of the electric field and q is the charge on the particle. For non-spherical particles traveling at low speed, the magnitude of the drag force can be approximated as $F_d = k(3\pi\mu)d_n v$ (McNown, et. al., 1951). Here k denotes the shape factor of the particle, μ is the dynamic viscosity of air, d_n is the particle's nominal diameter, and v is the velocity of the particle. Substituting these expresions into equations (1) and (2) gives

$$qE - k_x(3\pi\mu)d_n v\sin\theta = m\ddot{x} \qquad (3)$$

and

$$mg - k_y(3\pi\mu)d_n v\cos\theta = m\ddot{y} \qquad (4)$$

(v)sinq and (v)cosq are the horizontal and vertical components of particle velocity so that

$$qE - k_x(3\pi\mu)d_n \dot{x} = m\ddot{x} \qquad (5)$$

and

$$mg - k_y(3\pi\mu)d_n \dot{y} = m\ddot{y} \qquad (6)$$

Assuming the particle falls at terminal velocity v_T, the vertical component of acceleration is zero, and the vertical component of velocity is constant. Equation (6) then becomes $mg = k_y(3\pi\mu)d_n v_T$ which can be rearranged as

$$\frac{k_y}{m} = \frac{g}{(3\pi\mu)d_n v_T} \qquad (7)$$

If the particle rotates as it falls, the particle will have a random orientation with time. If we average k over time, the shape factor will be the same for all directions so that $k_x = k_y$. Dividing equation (5) by particle mass and substituting equation (7) for k_x/m gives

$$E\left(\frac{q}{m}\right) - \left(\frac{g}{v_T}\right)\dot{x} = \frac{d\dot{x}}{dt} \qquad (8)$$

Equation (8) expresses the motion of the particle in terms of the variables E and v_T (which can be measured experimentally) and the ratio q/m which we wish to determine. Equation (8) is solved by separation of variable. For brevity, we define the two constant expressions in equation (8) as E(q/m) = a and $(g/v_T) = b$. Substituting these expressions into equation (8), separating variables, and integrating both sides of the resulting expression gives

$$\int \frac{d\dot{x}}{a - b\dot{x}} = \int dt$$

or

$$T = \frac{1}{b} - 1n[a - b\dot{x}] + c_1 \qquad (9)$$

We evaluate the constant of integration c_1 by assuming the x - component of velocity is very small when the particle enters the electric field. At time t = 0, X=0 therefore $c_1 = \ln[a]/b$. Expression (9) becomes $t = -(1/b)\ 1n[(a-bx)/a]$. Exponentiating both sides this expression yields $1 - e^{-bt} = (b/a)\ x$, or

$$1 - e^{-bt} = \left(\frac{b}{a}\right)\frac{dx}{dt} \qquad (10)$$

Separating variables and integrating both sides of expression (10) gives $\int (1-e^{-bt})dt=(\frac{b}{a})\int dx$

or
$$t+(\frac{1}{b})e^{-bt}=(\frac{b}{a})x+c_2 \quad (11)$$

We evaluate the integration constant c_2 by defining the first known location of the particle as x = 0 at time t = 0. If we apply this boundary condition to equation (11), $c_2 = 1/b$, and $x=\frac{a}{b}[t+(\frac{1}{b})(e^{-bt}-1)]$

from which
$$a=\frac{b^2x}{[bt=(e^{-bt}-1)]} \quad (12)$$

Re-writing equation (12) in terms of the definition of a and b, and solving the expression for q/m gives

$$(\frac{q}{m})=\frac{(g/V_T)^2x}{E[(g/V_T)t+(e^{-gt/V_T}-1)]} \quad (13)$$

This equation is the basis of our experimental technique. It evaluates charge-to-mass ratio q/m, from measurements of deflection x, over time t, and the particle's terminal velocity v_T. Electric field strength must be known, and gravitational acceleration assumed constant.

EXPERIMENTAL METHODS

Apparatus

Figures 2 shows the experimental apparatus. Four subunits make up the device. The expansion chamber extracts particles from saltation, allowing some to fall into the extension tube, where they accelerate to terminal velocity. Only particles that pass through the detector enter the electric field chamber. The fourth sub-unit, the imaging system, is comprised of the detector, camera, and multi-strobes system. The purpose of this last unit is to illuminate and photograph the particles in the electric field chamber.

The expansion chamber slows air flow and allow particles to settle. Constructed of sheet metal, the expansion chamber maintains the same ratios as the smaller drift trap reported by Mellor (1960). The expansion chamber connects to the rest of the apparatus by means of a rotating cap. This allowed the direction of the nose cone inlet to be adjusted for different wind directions. Once positioned the cap was fixed in place and sealed by an adhesive fastener (duct tape).

The extension tube allows the particles to reach terminal fall velocity before entering the measurement region. Schmidt (1981) reports size distributions of saltating particles with mean equivalent diameters near 200 mm. Using a computer iteration scheme, we determined 24 cm is required for a 200 mm ice sphere to reach a terminal velocity of 53 cm/s. The vertical dimension of the extension tube was 55 cm in order to insure that most particles attained terminal velocity. The images provide a test of this requirement

The electric field chamber is sealed, providing a still air region. Two aluminum plates, (figure 2b) connected to high voltage power supplies, produce a horizontal electric field across a 20 cm plate separation. Leveling mechanisms on the bottom corners of the chamber allow leveling to set the electric field perpendicular to gravity. Flat black paint on all interior surfaces of the chamber reduce reflections, and black velvet on the chamber wall opposite the camera gives high contrast to the particle images. The high voltage supplies, adjustable over a range of 0-20 kV, provide a variable electric field. Plate voltage measured with a high voltage probe during the experiment were + 14.93 kV and -14.60 kV, giving an electric field strength E = 147.65 V/mm. Higher values interfered with the particle detection circuit.

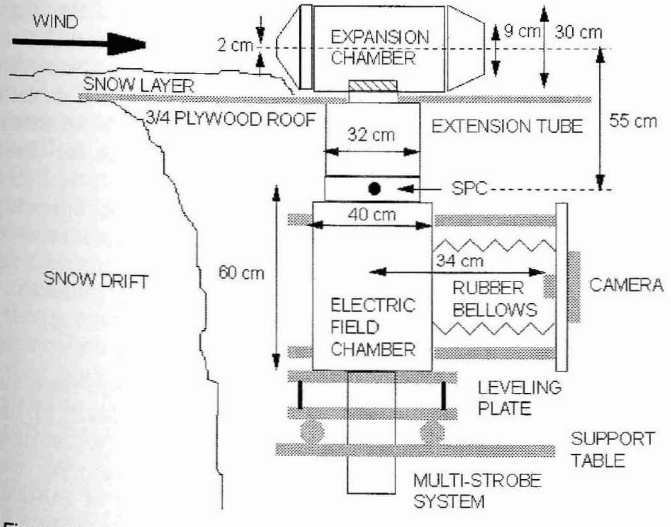

Figure 2a: Apparatus for measuring charge-to-mass ratios of individual blowing snow particles.

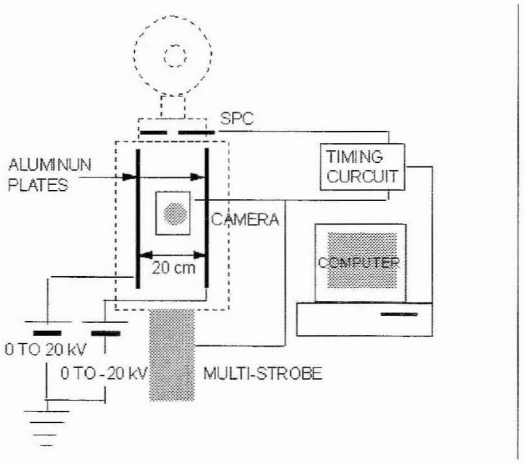

Figure 2b: Schematic diagram of electric field chamber and photo-imaging system.

The multi-strobe system (Bird and Jairell, 1989) provides continuous light from a halogen lamp, and accurately timed flashes from eight electronic strobes. The result is a photographic image showing a sequence of dots, defining particle location, along low intensity white streak on a black background. An adjustable slit (set to 1 cm), on a clear plastic window sealed to the bottom of the electric field chamber, confines illumination to a region perpendicular to the plates and centered in the chamber. A small fan on the multi-strobe housing removes heat produced by the halogen lamp.

The timing circuit performs two functions. It opens the camera shutter when a particle is detected, and triggers the strobe sequence after a delay that allows the particle to move from the detector into the electric field chamber. Particles are detected by a snow particle counter (SPC) that senses the particles shadow in a light beam (Schmidt, 1977). We used a 35-mm film camera with motor drive, data back, and 55-mm, f 1.4 lens to record particle images. A microprocessor controls the timing circuit, allowing programmable time delays. For our experiment, a time delay of 121.6 ms was set between particle detection and first strobe flash, with 20.0 ms intervals between each flash.

Field Procedure

The experiment was conducted on 8 January 1996 at the Chimney Park trailhead, 96 km west of Laramie, Wyoming on Highway 130. Snowplow operators for the Wyoming Highway Department assisted us in forming a 2.1 m high snow bank, at the west end of the trail head parking lot. Suitable snow cover existed upwind of the site, though no new snow had fallen in several days. A mobile laboratory provided electricity and shelter for computers (as well as investigators). Supporting meteorological data included wind speed and direction, air temperature, and humidity, all measured 1 m above the surface near the top of the snowbank.

The apparatus was set up in the parking lot just downwind of the snowbank. A roof, level with the top of the snowbank, prevented the apparatus from being drifted in (Fig. 2a). A 20-cm layer of snow, placed on the roof, smoothed the approach to the inlet of the device. The electric field chamber was leveled and the inlet aligned with the wind.

A length scale was defined for image analysis by suspending a section of metric ruler at the center of the field of view for the first two pictures of each film roll. Four rolls of 36 exposure (ASA 1600) were exposed between 1400 and 1700-h, in low-level drifting (no noticeable suspension).

Analysis Procedure

Figure 3: Image showing trajectories of the first four particles in Table 1. Strobe number five failed to flash throughout the experiment. The image was enhanced and converted to black and white for this figure. Continuous traces were converted to black in the process.

Of the 136 images we exposed, 50 showed particle images. We transferred these to compact disk for analysis using computer software. Figure 3 shows an example image from which particle location was digitized. We also digitized the endpoints of the same100-mm segment in all images of the ruler, to determine a length scale.

Vertical distance between dots, divided by the 20-ms strobe interval, determined particle fall velocity. If the particle was at terminal velocity, an average value was computed for v_T. Horizontal distance between the first and last dot on the path determined horizontal deflection, x. The time, t, for this deflection was the product of the 20-ms strobe interval and the number of intervals between the first and last dot. These measured values of vT, x, and t, together with E = 147.65-kV/m, and g = 9.81-m/s^2 provide the arguments required to evaluate the charge-to-mass ratio of the particle using equation (13)

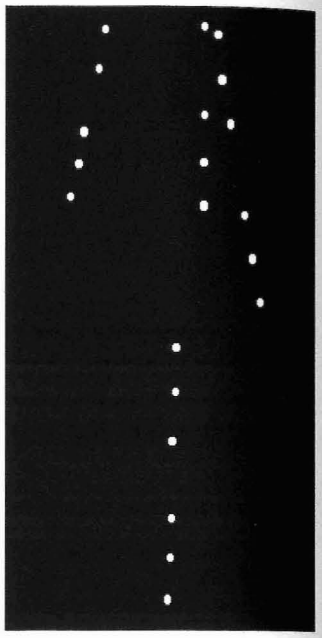

Figure 3: Image showing trajectories of the first four particles in Table 1. Strobe number five failed to flash throughout the experiment. The image was enhanced and converted to black and white for this figure. Continuous traces were converted to black in the process.

In selecting particle traces for analysis, two criteria were used to ensure particles were traveling at terminal velocity, and that measured deflections resulted only from the electrostatic force: (a) At least three strobe dots had to be visible to check for terminal velocity. (b) A trace could not approach or cross other trajectories, to be certain the deflection was not influenced by other particles.

EXPERIMENTAL RESULTS

The largest variation in measured distance on the eight ruler images was less then 1%, therefore we used the average of 419 du/mm to convert coordinates of the strobe dots from digitizer units (du) to actual distance in mm. 11 traces met the criteria for analysis. Table 1 list measurements and computed charge-to-mass ratios for these particles. Data for the four particles in figure 3 is listed first. Wind speed decreased from 10-m/s at the beginning of sampling to 5-m/s near the end. Temperature decreased from +1°C to -2°C, with relative humidity dropping from 93% during peak drifting, to 70% as winds decreased.

Error Analysis

We estimated the errors for computed charge-to-mass ratios in Table 1 from the errors in each argument of the computation. Table 2 lists these values. A worst-case analysis for a particle with 500-mm/s fall velocity, deflected 15-mm in 100-ms by an electric field of 148-kV/mm gives a maximum error of 4% in q/m, equal to 1.5-μC/kg. Percent error increased as deflections decreased.

DISCUSSION

The derivation of equation (13) depends on two critical assumption. (a) Particles fall at terminal velocity, and (b) the shape factor (drag coefficient) is the same in all directions. Very consistent vertical distances between dots on each trace strongly support both assumptions. Measured variations in fall velocity were random for all traces, and within the uncertainty of the measurement. We saw no trace oscillations characteristic of particles falling with a preferred orientations (as reported for plate snow crystals, for example). The ratio of longest axis to perpendicular axis averaged 1.49 for saltating snow photographed by Schmidt (1981). Saltation impacts and non-uniform instantaneous drag on such particles will cause rotations that continue after particle's enter our apparatus. These rotations should yield an average shape factor approximately constant with respect to direction.

ticles with negative charge saltating on a snow surface with net positive charge, the electrostatic force (attraction) shortens trajectories. On the other hand, particles with positive charge, eroded from the surface during wind gust, should have longer trajectories with higher rebounds. These particles will have increased probability of suspension by turbulence. Based on the results reported here, questions of charge distribution with height, and charge decay rate for particles freshly detached from the surface, become critical next steps in our research.

CONCLUSIONS

Although the apparatus is necessarily large, modification of Millikan's (1910) technique can provide charge-to-mass ratios for individual saltating particles.

TABLE 1: MEASUREMENTS AND COMPUTED CHARGE-TO-MASS RATIOS

PARTICLE NUMBER	v_T (mm/s)	StdDev v_T (mm/s)	x (mm)	t (ms)	q/m (μC/kg)
1	425.18	5.35	-14.53	100	-37
2	534.69	19.56	0.38	100	1
3	557.93	18.32	19.12	120	33
4	534.61	0.00	-1.15	40	-12
5	510.13	0.13	13.74	100	32
6	338.17	10.06	11.91	120	27
7	571.38	18.24	22.61	80	72
8	593.55	11.86	-11.91	120	-20
9	491.87	12.84	-26.27	100	-63
10	438.78	14.34	-18.63	40	-208
11	627.45	7.09	-10.08	40	-106

Average charge-to-mass ratios near -10 μC/kg were reported for blowing snow in the semi-arid climates of Montana (Latham and Montagne, 1970) and Wyoming, USA (Schmidt, 1994). Ratios as large as -50 μC/kg were measured in Antarctica by Whishart (1969). Most of the particles we evaluated had charge-to-mass ratios significantly higher then average charge-to-mass ratios previously measured in semi-arid climates. The largest individual ratio was -208 μC/kg, four times the largest average ratio previously reported. Although knowledge of the electrification process in incomplete, we speculate that even larger ratios occur in more intense drifting. Schmidt (1994) demonstrates that a charge-to-mass ratio of -10 μC/kg has a significant influence on computed saltation trajectories. For particles with negative charge saltating on a snow surface with net positive charge, the electrostatic force (attraction) shortens trajectories. On the other hand, particles with positive charge, eroded from the surface during wind gust, should have longer trajectories with higher rebounds. These particles will have increased probability of suspension by turbulence. Based on the results reported here, questions of charge distribution with height, and charge decay rate for particles freshly detached from the surface, become critical next steps in our research.

Blowing snow particles with opposite charge sign coexist in saltation. This fact must be considered when measurements of charge-to-mass ratios are made by averaging the charge over a sample mass.

Even for the low-intensity drifting in this experiment, particle charge-to-mass ratios were significantly larger then the maximum q/m previously estimated by trapping weighable quantities of drifting particles in a Faraday cage.

TABLE 2: ERROR SOURCE IN CHARGE-TO-MASS COMPUTATIONS

SOURCE OF ERROR	ERROR IN MEASUREMENT	CONTRIBUTION TO ERROR IN q/m
TIME INTERVAL t	± 0.4 ms	NEGLIGIBLE
DEFLECTION x	± 0.6 mm	2%
FALL VELOCITY v_T	± 15.3 mm/s	1%
ELECTRIC FIELD E	+1,-2 V/mm	1%

REFERENCES

Bird, K.G. and Jairell, R.L. 1989. Sequential Flash for Photographing Trajectories of Saltating Snow Particles. Prec. 57th Western Snow Comference, Apr 18-20, 1989, Fort Collins. CO., USA.

Camp, P.R. 1976. Charge, Morphology, and pH of Natural Snow. J. Geophys. Res., 81(9), 1589-1592.

Johnston, A.R. and Kirkham, H. 1989. A Miniaturized Space-Potential DC Electric Field Meter. IEEE Trans Power Deliv., 4(2), 1253-1261.

Latham, J. and Montagne, J. 1970. The possible importance of electrical forces in the development of cornices. J. Glaciol., 9(57), 375-384.

McNown, J.S., Malaika, J., and Pramanik, R. 1951. Particle Shape and Settling Velocity. Trans. 4th Meeting of the International Association for Hydraulic Research, Bombay India, 1951, pp 511-522.

Mellor, M. 1960. Gauging Antarctic Drift Snow. Antarctic Meteorology, Pergamon Press, New York, 1960.

Millikan, R.A. 1910. Electrons, Protons, Photons, Neutrons, Mesotrons, and Cosmic Rays, 2ND edition. University of Chicago Press, Chicago, 1947.

Schmidt, R.A., 1977. A System That Measures Blowing Snow. U.S. For. Serv. Rocky Mt. For. Range Exp. Stn. Res. Pap., RM-194.

Schmidt, R.A., 1981. Estimating Threshold Windspeeds From Particle Sizes in Blowing Snow. Cold Reg. Sci. Technol., 4, pp. 187-193.

Schmidt, S. and Dent, J.D. 1993. A Theoretical Prediction of the Effects of Electrostatic Forces On Saltating Snow Particles. Ann. Glaciol., 18, 234-238.

Schmidt, S. 1994. Measurements Of The Electric Field Gradient In a Blizzard. Proc. International Snow Science Workshop, Oct. 30-Nov.3, 1994, Snowbird, UT, USA. pp 197-202.

Schmidt, S. and Schmidt R.A. 1992. The Sign Of Electrostatic Charge On Drifting Snow. Proc. International Snow Science Workshop, Oct 4-8, 1992, Breckenridge, CO, USA. pp. 351 - 360.

White, B. and Schultz, J. 1977. Magnus effects in saltation. J. Fluid Mech., 81(3), 495-512.

Wishart, E. R. 1968. Electrification of Antarctic drifting snow. Proc. Int. Symposium Antarctic Glaciological Exploration, Sept. 3-7, 1968, Hanover, NH, USA. IASH Pub.